Concurrent higher-order field monitoring eliminates thermal drifts in parallel DWI

B. J. Wilm[1], C. Barmet[1], C. Reischauer[1], and K. P. Pruessmann[1]
[1]Institute for Biomedical Engineering, University and ETH Zurich, Zurich, Zurich, Switzerland

Introduction: Diffusion-weighted imaging often requires perfect congruence among a set of variably diffusion-weighted (DW) images, e.g., to calculate diffusion tensors. Even minute geometrical mismatches can impose large errors in derived data such as probability density, fractional anisotropy (FA), or fiber tractograms. However, DWI is notoriously prone to image incongruence. One source of image distortions are eddy-current induced fields caused by strong diffusion gradients. The other major cause of geometric inconsistency is temperature-related field drift induced by a diffusion scan itself or by a preceding gradient-intensive exam such as fMRI.

Typically these problems are mitigated by image co-registration. Yet a generally suitable deformation model is hard to determine and the inherently low signal-to-noise-ratio of diffusion data can cause poor performance of co-registration. Alternatively, dynamic field imperfections can be accounted for in image reconstruction if they are known with high accuracy. In diffusion imaging, eddy-current effects up to third order in space have been successfully addressed in this way, relying on separate field evolution measurements with an NMR field camera [1,2]. To extend this approach to thermal effects, higher-order field measurements must be performed simultaneously with the acquisition of image data, which is challenging due to mutual RF interference of the two concurrent experiments. In the present work this problem is solved by using ^{19}F NMR for a 16-channel field camera, which is naturally decoupled from ^{1}H diffusion imaging. In addition, higher-order image reconstruction has been extended to support parallel imaging for shortening TE and reducing susceptibility artifacts.

Methods: All experiments were performed on a 3T Achieva system (Philips Healthcare, Best, NL). Sixteen transmit/receive ^{19}F NMR probes based on droplets of hexafluorobenzene (C_6F_6) were mounted on an 8-channel ^{1}H head receiver array. DWI was performed with single-shot spin-echo EPI in a spherical silicone oil phantom (ø=20cm) and in a healthy volunteer. The field probes were generally excited after the second diffusion gradient. Fluorine and proton signals were then acquired simultaneously via 24 channels of the system spectrometer. Diffusion weighting (b=1000mm^2/s) was applied in 6 orientations along with non-DW (b_0) reference data. The scan parameters were (in-vitro/in-vivo): TE=84/75ms, TR=5000ms,

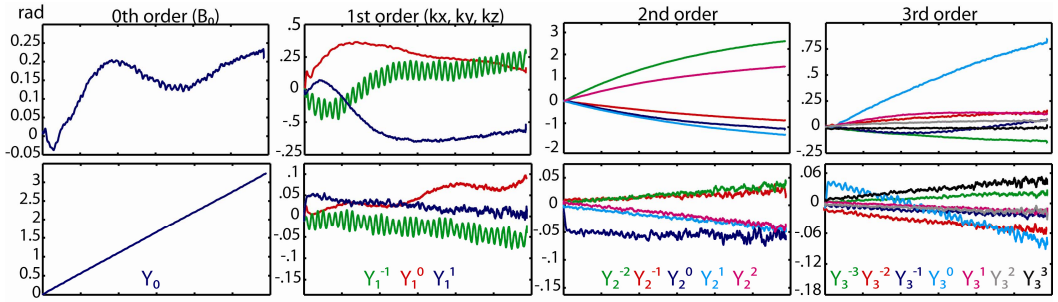

Fig. 1, Top: Effect of diffusion gradients on field dynamics during the subsequent signal readout (43ms), as reflected by concurrently measured phase coefficients. Bottom: Differences between a 1st and 3rd average reflect thermal drifts. All plots are scaled to show maximum phase within the imaging volume relating to each spherical harmonic basis function Y_l^m.

76/42(SENSE R=3) phase encodes, readout duration=43.3/31.6ms, FOV=230mm, 3/8 averages. The phase of the probe signals was used to fit a 3rd-order spherical-harmonic phase model [2], describing the field evolution and thereby the spatial encoding during the entire readout. This model was then used as the basis of higher-order image reconstruction with a conjugate gradient algorithm [2], which was extended to encompass parallel imaging by incorporating coil sensitivities in the encoding matrix.

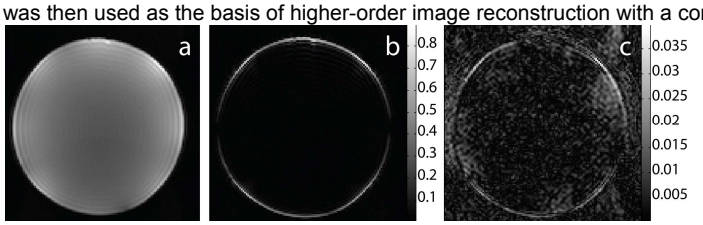

Fig. 2: Difference between 1st (a) and 3rd average normalized to the maximum image value when (b) neglecting and (c) accounting for thermal

Results: Figure 1 displays sample results of concurrent field monitoring during the EPI readout. Eddy-current effects are highlighted in the top row, showing differences of coefficient time-courses obtained with and without diffusion weighting. The bottom row illustrates thermal effects, showing differences between the first and third repetitions of a given phantom scan. Neglecting these drifts resulted primarily in image shifts in the phase encoding direction, reflecting the dominant 0th-order effect seen in Fig. 1. The shift of about 3mm is evident in Fig. 2, showing the first image (Fig. 2a) along with the difference between the first and the third (Fig. 2b) when reconstructing both with the same field model. Conversely, virtually perfect congruence is achieved when reconstructing both images with their individual, concurrently measured field information (Fig. 2c). Similarly, in-vivo images obtained with monitoring-based higher-order reconstruction showed no visible distortion or relative shifts between any of the different repetitions and diffusion weightings (Fig. 3). This congruence permitted, without co-registration, straightforward averaging and calculation of derived data such as a mean DWI (Fig. 3b), apparent diffusion coefficient (ADC) (Fig. 3c) and FA maps (Fig. 3d-e).

Discussion and Conclusion: Concurrent field monitoring captures the full field dynamics during each DWI acquisition. By integrating this information into image reconstruction it is now possible to eliminate the effects of thermal drifts along with those induced by eddy currents and other gradient imperfections. The resulting geometric congruence of variably diffusion-encoded data facilitates data processing and is expected to improve the accuracy and effective resolution of derived parameter maps. Unlike previous, separate implementations, concurrent field monitoring does not require any additional scan time or any assumptions on the reproducibility of field dynamics. It thus holds equal promise for other quantitative MR methods such as fMRI, spectroscopy, and phase-contrast imaging. Finally, this work is the first report of parallel imaging with higher-order reconstruction, illustrating the versatility that reliable knowledge of field dynamics lends to algebraic reconstruction approaches.

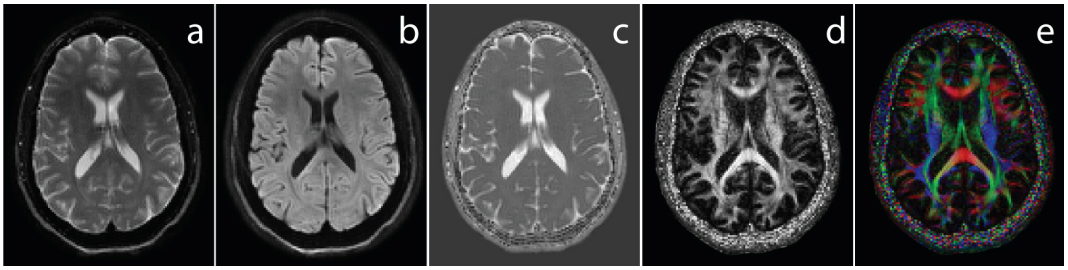

Fig. 3: Parallel DTI with concurrent field monitoring and higher-order reconstruction. a: T_2-weighted (b_0), b: mean DW, c: ADC, d: FA, e: color-coded FA.

References:
[1]:Barmet et.al ISMRM'09;p.780
[2]:Wilm et al.ISMRM'09; p.562